Title
Engineering yeast for the de novo synthesis of jasmonates

Journal
Nature Synthesis, 3(2)

ISSN
2731-0582

Authors
Tang, Hongting
Lin, Shumin
Deng, Jiliang
et al.

Publication Date
2024-02-01

DOI
10.1038/s44160-023-00429-w

Engineering yeast for de novo synthesis of jasmonates

Hongting Tang[1,2,3 †,*], Shumin Lin[1,2,3†], Jiliang Deng[1†], Xiaozhou Luo[1,2,3*], Jay D. Keasling[3,4,5,6,7*]

[1]Shenzhen Key Laboratory for the Intelligent Microbial Manufacturing of Medicines, Shenzhen Institute of Advanced Technology, Chinese Academy of Sciences, Shenzhen, 518055, CN
[2]CAS Key Laboratory of Quantitative Engineering Biology, Shenzhen Institute of Synthetic Biology, Shenzhen Institute of Advanced Technology, Chinese Academy of Sciences, Shenzhen, 518055, CN
[3]Center for Synthetic Biochemistry, Shenzhen Institute of Synthetic Biology, Shenzhen Institutes of Advanced Technology, Chinese Academy of Sciences, Shenzhen 518055, CN
[4]Joint BioEnergy Institute, Emeryville, California 94608, United States
[5]Biological Systems and Engineering Division, Lawrence Berkeley National Laboratory, Berkeley, California 94720, United States
[6]Department of Chemical and Biomolecular Engineering & Department of Bioengineering, University of California, Berkeley, California 94720, United States
[7]Novo Nordisk Foundation Center for Biosustainability, Technical University of Denmark, Kgs. Lyngby 2800, Denmark
[*]Corresponding author: E-mail: ht.tang@siat.ac.cn (H.T.); xz.luo@siat.ac.cn (X.L.); jdkeasling@lbl.gov (J.K.)
[†]These authors contributed equally to this work.

Abstract

Jasmonates are a class of plant hormones with many agricultural applications and potential medicinal properties. However, the low content of jasmonates in plants and environmental issues with their production make their supply challenging. Here, we completed the de novo microbial biosynthesis of jasmonic acid (JA) and its derivatives, methyl jasmonate and jasmonoyl-isoleucine, from glucose using an engineered baker's yeast. The study employed enzymes located in the endoplasmic reticulum and cytosol to generate intermediates α-linolenic acid and *cis*-12-oxophytodienoic acid. Our final engineered stain, which integrates 15 heterologous genes from diverse plants and fungi and had three of its native genes deleted, produces JA at titers of 19.0 mg/L in flask cultures through in vitro supplementation of α-LeA. In addition to the well-known natural structures (-)-JA and (+)-epi-JA, the engineered yeast also synthesized the previously unobserved unnatural structures (+)-JA and (-)-epi-JA. These results demonstrate that yeast is a clear, scalable, and sustainable platform to produce both naturally occurring jasmonates as well as those structures not found naturally in plants.

Introduction

Jasmonic acid (JA) and its derivatives are collectively called jasmonates. They are an essential class of hormones that are ubiquitously present in plants, regulating their growth, development, and response to biotic or abiotic stress. Jasmonates are environmentally friendly compounds that have gained popularity in agriculture due to their ability to enhance crop yields and boost plant stress tolerance. They are also an attractive alternative to replace traditional

chemical pesticides by boosting plant defense against pests and pathogens[1]. Additionally, jasmonates can be used to induce the biosynthesis of natural products with important clinical value, such as paclitaxel and camptothecin[2, 3]. Moreover, jasmonates play an essential role in the perfume industry, particularly for production of high-grade perfumes, detergents, shampoos, cigarettes, and floral foods, because of their distinct jasmine scent[4, 5]. It is worth noting that jasmonates are structurally similar to prostaglandins, and studies have reported their pharmacological anticancer activity, which could have potential for cancer treatment[6-8]. Traditionally, jasmonates are extracted from plants; however, due to their extremely low concentrations, typically ranging from 10 to 100 ng/g of fresh weight, the commercial production of jasmonates can be costly and the extraction process is environmentally hazardous[9, 10]. Consequently, numerous efforts have been exploited to synthesize jasmonates chemically, but this approach has proven to be labor-intensive and low yielding in industry[11]. Recent advances in synthetic biology have enabled an attractive route for the production of valuable chemicals, namely microbial cell factories[12]. Although some fungal species, such as *Diplodia* and *Lasiodiplodia*, have been found to produce jasmonates, no microbial production of jasmonates has been sufficiently economical for industrial use due to the presence of malodorous compounds and allergens that pose safety challenges and require complex purification processes[13]. Moreover, the unclear genetic information, limited tools for genetic manipulation, and difficulties in scaling up production make these fungal species difficult and labor-consuming to engineer for improving production of jasmonates.

Saccharomyces cerevisiae, recognized as a Generally Recognized as Safe (GRAS) chassis organism, has been widely used for industrial production of biochemicals[14, 15]. It is a well-studied organism with genetic tractability and can be edited quickly and robustly using available genetic tools, such as the CRISPR/Cas9 technology, to produce the desired products[16-18]. Its robustness to fermentation conditions makes it compatible with large-scale cultivation in bioreactors[19]. Most importantly, it harbors various organelles—cytosol, mitochondrion, peroxisome, endoplasmic reticulum (ER) and vacuole—that are essential for reconstitution of plant pathways with multiple enzymes with different native locations. Therefore, *S. cerevisiae* is the preferred cell factory for production of jasmonates, which have not been reconstituted in genetically tractable heterologous microbial hosts.

In plants, JA biosynthesis is initiated from α-linolenic acid (α-LeA) synthesized by fatty acid desaturase (FAD) on the chloroplast membrane, which is then released from galactolipids by phospholipase I (Fig 1). An enzyme complex consisting of 13-lipoxygenase (LOX), allene oxide synthase (AOS) and allene oxide cyclase (AOC) catalyzes the conversion of α-LeA into the intermediate *cis*-12-oxophytodienoic acid (OPDA) in the chloroplast[20]. OPDA is exported into the cytosol by a protein called JASSY[21], then imported into the peroxisome by the ABC transporter Comatose on the peroxisomal membrane[22]. In the peroxisome, OPDA reductase (OPR) catalyzes reduction of the cyclopentenone ring, and the carboxylic acid side chain of JA is shortened by a β-oxidation process. This process is catalyzed by several enzymes including acyl-CoA synthetase (ACS), acyl-CoA oxidase (ACX), multifunctional protein (MFP) which contains 2-trans-enoyl-CoA hydratase and L-3-hydroxyacyl-CoA dehydrogenase activities, and L-3-ketoacyl CoA thiolase (KAT)[23]. The formed JA enters the cytosol to produce a diversity of derivatives. Therefore, JA biosynthesis is a complex, multi-enzyme catalyzed process that exhibits extensive compartmentalization, with enzymes active across the chloroplast,

peroxisome, and cytosol. The chloroplast is the compartment for production of the precursors α-LeA and OPDA. As yeast does not have a chloroplast, reconstitution of the JA pathway presents a challenge due to the incompatibilities of enzymes adapted for unusual contexts.

In this study, we developed a de novo synthetic pathway for JA biosynthesis in *S. cerevisiae*. Once established, we improved α-LeA production 30-fold through engineering fatty acid metabolism and increasing the copies of synthetic enzymes. We then screened and selected three active LOXs from six candidates by removing their localization peptides and optimized their expression, leading to a titer of 10.8 mg/L of 13-HPOT, a precursor of OPDA. OPDA production was then realized in the cytosol by expressing AOS and AOC without chloroplast localization peptides. De novo JA synthesis from glucose was finally completed by locating a series of plant enzymes in the yeast peroxisome. Our final strain involved the disruption of three native biosynthetic enzymes, the introduction of 15 heterologous enzymes derived from diverse plants and fungal species, and optimization of cultivation conditions with in vitro supplementation of α-LeA to produce JA at titers of 19.0 mg/L from glucose in flask cultures. In addition, we produced JA derivatives, including methyl jasmonate (MeJA) and jasmonoyl-isoleucine (JA-Ile), at comparable levels to JA. Our engineered stains represent a significant step towards the large-scale and sustainable production of jasmonates.

Results

Design of jasmonates biosynthesis in yeast

Based on the substrate/production locations in the plant, the jasmonates synthetic pathway that was refactored in *S. cerevisiae* was divided into four modules (Fig 1). *S. cerevisiae* cannot naturally generate α-LeA, even though it can synthesize its precursor, oleic acid, in the endoplasmic reticulum (ER). Some other yeast and plant seeds can produce α-LeA in the ER. Several FADs from them have been functionally expressed in *S. cerevisiae* and characterized, which resulted in the production of α-LeA[24-28]. Therefore, we engineered *S. cerevisiae* for efficient biosynthesis of α-LeA in the ER as Module I. As there is no chloroplast in yeast and de novo OPDA biosynthesis has not been reported in yeast, it was necessary to select a proper compartment for OPDA synthesis in *S. cerevisiae* to complete JA biosynthesis. There are two potential candidates: the peroxisome, which is the location of JA biosynthesis in plants and requires no additional OPDA transport, and the cytosol, which only requires OPDA transport from the cytosol into the peroxisome. However, fatty acids are degraded in the peroxisome, which may reduce accumulation of α-LeA for OPDA synthesis. Therefore, OPDA biosynthesis was localized to the cytosol, which constituted Module II. Reduction and β-oxidation of OPDA take place in plant peroxisomes, which have conserved functions in eukaryotic organisms including yeast[29]. Therefore, we constructed JA biosynthesis in the peroxisome mimicking plants (Module III). Finally, JA was converted into various functional derivatives in the cytosol, including MeJA and JA-Ile (Module IV).

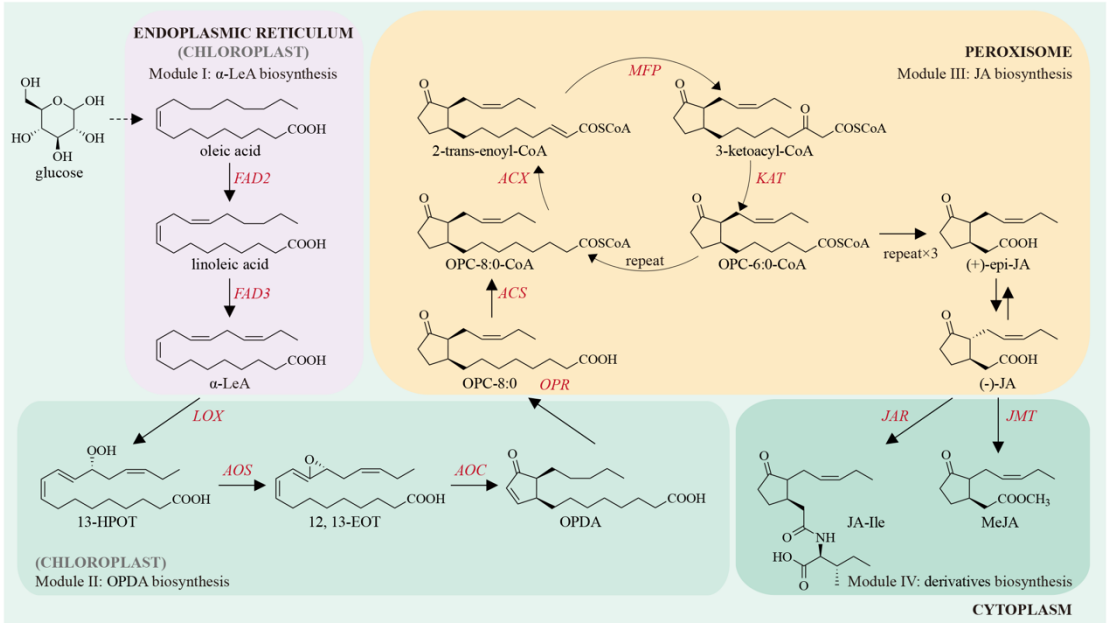

Fig 1 Engineering biosynthetic pathway for de novo production of jasmonates in *S. cerevisiae*. Abbreviations are defined in the text. The colored boxes indicate the four divided modules. Module I is α-LeA biosynthesis in the ER (pink). Module II is OPDA biosynthesis in the cytosol (green). Module III is JA biosynthesis in the peroxisome (yellow). Module IV is JA derivatives biosynthesis in the cytosol (dark green). Gray words in brackets indicate the plant organelles for intermediates synthesis. All genes marked with red represent expressed heterologous genes.

Efficient biosynthesis of α-LeA in the ER

S. cerevisiae is capable of naturally producing oleic acid, which serves as a precursor for α-LeA biosynthesis. For efficient biosynthesis of α-LeA in the ER, we introduced two heterologous enzymes: Δ12 fatty acid desaturase (FAD2) to convert oleic acid into linoleic acid and ω3 fatty acid desaturase (FAD3) to convert linoleic acid to α-LeA. *Kl*FAD2 and *Kl*FAD3 from *Kluyveromyces lactis* have been previously expressed on high-copy plasmids in *S. cerevisiae* to study the biological significance of α-LeA[24, 30, 31]. As plasmid expression is unstable, we integrated *Kl*FAD2 and *Kl*FAD3 into the genome to create strain SJ01 (Fig S1). SJ01 was cultivated in nitrogen-limited minimal (NSD) medium at 25 ℃ for 7 days to produce linoleic acid and α-LeA, which resulted in its higher production of fatty acids compared to the standard synthetic complete medium[32]. Linoleic acid and α-LeA were detected (Fig 2A), albeit at very low titers of 2.3 mg/L and 0.7 mg/L, respectively (Fig S2). We also observed that the wild-type strain and SJ01 produced only approximately 12.0 mg/L oleic acid (Fig S3). To increase α-LeA production, we optimized the cultivation conditions, as previously reported, including the culture medium, cultivation temperature, and cultivation time[30]. After optimization, we were able to increase the production of α-LeA to 1.6 mg/L when cultured in YPD medium at 25 ℃ for 5 days (Fig S4A), and the production of linoleic acid and oleic acid also increased (Fig S4B and Fig S4C). However, the production of α-LeA remained too low to proceed with downstream steps of the JA synthetic pathway.

The expression of heterologous enzymes in a host organism can be challenging due to improper intracellular localization, resulting in low enzymatic activity and reduced product yield. To determine whether *Kl*FAD2 and *Kl*FAD3 fused with their native ER localization

peptides could be correctly anchored to the yeast ER membrane, which has not been previously studied, we fused each enzyme with the red fluorescent protein mCherry. To confirm the ER membrane localization of the enzymes, we used enhanced green fluorescent protein (eGFP) fused with an ER membrane localization peptide as a positive control[16]. Although the red fluorescence was relatively weak, we observed that it co-localized with the green fluorescence (Fig 2B), indicating that both enzymes were correctly located on the ER membrane.

Although FAD2 and FAD3 are typically known to act on lipid-linked substrate phospholipids[33], the production of linoleic acid has been shown to increase when a *Kl*FAD2-expressing strain was grown in the presence of exogenous oleic acid as a substrate[24]. Exogenous linoleic acid has also been shown to be converted into α-LeA when *Kl*FAD3 was expressed[24]. These results suggest that increasing free fatty acids may be used for the synthesis or turnover of phospholipids, which can then facilitate the synthesis of linoleic acid and α-LeA. Therefore, we implemented several metabolic engineering strategies to enhance the biosynthesis of free fatty acids[34], which in turn should increase the production of α-LeA (Fig 2C). The thioesterase 'tesA from *Escherichia coli*, which is specific for saturated and unsaturated fatty acyl thioesters of chain length C_{14} to C_{18}[35], was expressed to promote the conversion of fatty acyl-ACP into free fatty acids, while the fatty-acyl coenzyme A oxidase Pox1p and fatty acyl-CoA synthetases Faa1p/4p were blocked to reduce the consumption of free fatty acids. The deletion of *FAA1/4* with expression of *'tesA* led to a remarkable 19-fold increase in the production of α-LeA, up to 30.2 mg/L, in SJ02 compared to the parent strain SJ01 (Figure 2D). Subsequent deletion of *POX1* further improved the production of α-LeA by 1.15-fold in SJ03. The production of linoleic acid and oleic acid in SJ03 was 23.9 mg/L and 279.9 mg/L, respectively (Fig S5A and S5B). However, the low conversion of oleic acid and its massive accumulation suggested that the insufficient activities of FAD2 and FAD3 were the rate-limiting steps.

To enhance FAD2 and FAD3 activities, we introduced additional copies of *Kl*FAD2 and *Kl*FAD3, driven by the strong constitutive promoters P_{TDH3} and P_{CCW12}[36], respectively, into the SJ03 genome, resulting in strain SJ04. This led to a 38.4% increase in α-LeA production in SJ04 relative to the parent strain SJ03, but it did not affect linoleic acid levels (Fig 2D and Fig S5A), indicating that the extra copy of *Kl*FAD3 can efficiently transform the additional linoleic acid when an extra copy of *Kl*FAD2 was engineered into the cell, as judged by the fact that we did not observe accumulation of linoleic acid. Interestingly, the expression of *Cs*FAD2 and *Cs*FAD3 from *Camelina sativa* in *S. cerevisiae* resulted in a higher α-LeA to total fatty acid ratio[27], suggesting their potentially superior activity over *Kl*FAD2 and *Kl*FAD3. Therefore, we explored the possibility of combining *Kl*FAD2 and *Kl*FAD3 with *Cs*FAD2 and *Cs*FAD3. Fluorescence imaging confirmed successful ER membrane localization of *Cs*FAD2 and *Cs*FAD3 (Fig S6). The introduction of *Cs*FAD2 and *Cs*FAD3, creating SJ05, resulted in a 47.5% improvement in α-LeA production, reaching a titer of 51.2 mg/L. Additionally, it led to a 40.1% increase in linoleic acid production (Fig 2D and Fig S5A). As expected, oleic acid production decreased in SJ05 (Fig S5B). These results indicate that the combined use of *Kl*FAD2/3 and *Cs*FAD2/3 was slightly more effective than simply increasing the copies of *Kl*FAD2 and *Kl*FAD3 and can avoid homologous recombination through the repeated use of the same genes. Additionally, we expressed *Rn*ELO2 from *Rattus norvegicus*, which converts C_{16} to C_{18} fatty acids[37] (Fig S7A), to increase oleic acid production and further improve α-LeA yield. However, introduction of *Rn*ELO2 only increased oleic acid production but decreased palmitoleic acid

levels (Fig S7B), without affecting linoleic acid or α-LeA production (Fig S7B).

Linoleic acid and α-LeA are produced from phospholipids, and thus they may be present in membranes. We conducted an analysis of the cell membrane components to ascertain the presence of linoleic acid and α-LeA. We found linoleic acid and α-LeA in the membranes of strain SJ05, but not in the wild-type strain (Fig S8). Additionally, lipidomics analysis was conducted to characterize the constituents of phospholipids, including phosphatidic acid (PA), phosphatidylinositol (PI), phosphatidylserine (PS), phosphatidylethanolamine (PE), phosphatidylglycerol (PG) and phosphatidylcholine (PC). We found linoleic acid and α-LeA in phospholipids (Table S1), indicating their presence in the membrane of strain SJ05. To assess the effects of α-LeA production on the cell phenotype, several experiments were performed. Growth curves were measured, and we found that SJ05 grew slower compared to the wild-type strain (Fig S9A). The specific growth rate of SJ05 was 0.147 h^{-1}, while the wild-type strain exhibited a rate of 0.209 h^{-1} (Fig S9B). No significant differences in tolerance to temperature and ethanol were observed between the wild-type strain and SJ05 (Fig S9C and S9D).

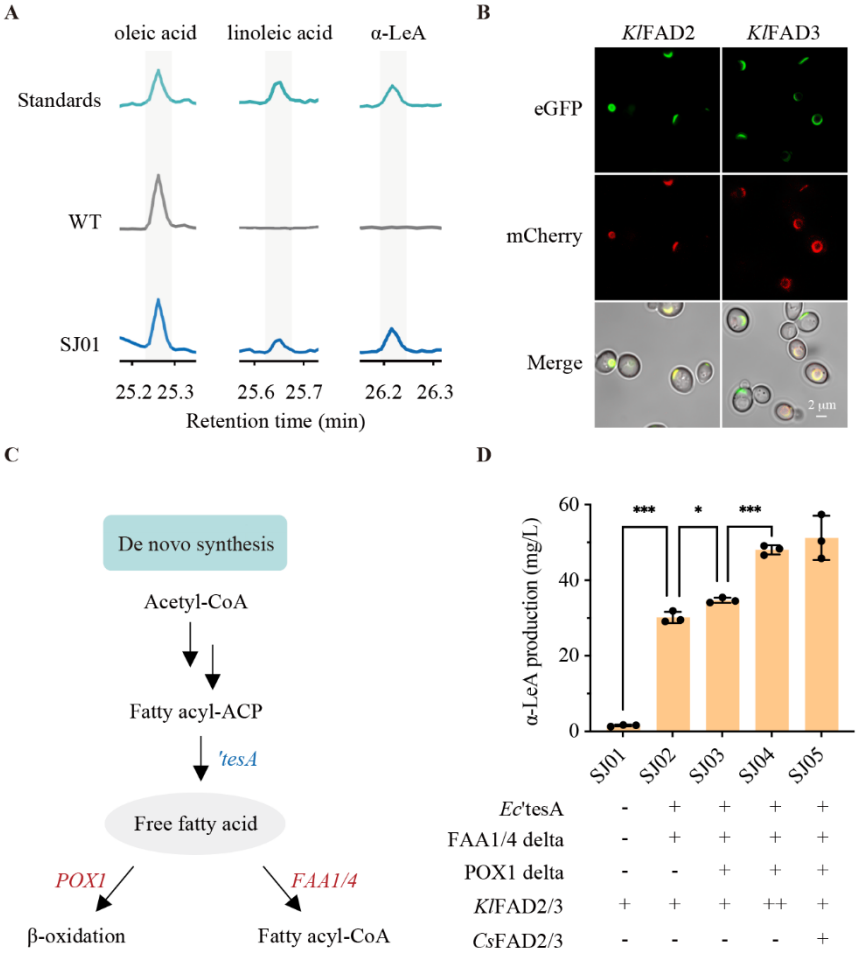

Fig 2 Engineering for efficient production of α-LeA. A. SJ01 produced linoleic acid and α-LeA from glucose. B. Localization of FAD2/FAD3 on the ER membrane. C. Metabolic engineering of the fatty acid biosynthesis pathway. D. Increase in α-LeA production by engineering fatty acid biosynthesis pathway and introducing an additional copy of FAD2/FAD3. WT, wild-type stain. Statistical analysis was performed using one-tailed Student's t-test (*$p < 0.05$, ***$p < 0.001$). All data are presented as mean ± SD of biological triplicates.

Engineering cytosolic OPDA biosynthesis

Having optimized the de novo production of α-LeA, our next goal was to construct an OPDA biosynthesis pathway by expressing the lipoxygenase (LOX), allene oxide synthase (AOS), and allene oxide cyclase (AOC) enzymes in the yeast cytosol. The de novo heterologous biosynthesis of OPDA has not been reported. Thus, we selected *At*LOX2, *At*AOS, and *At*AOC2 from *Arabidopsis thaliana*, which is a well-known model for the study of the JA synthetic pathway[38], to create a yeast OPDA biosynthesis pathway. The chloroplast localization peptides of *At*LOX2 (1-56 amino acids), *At*AOS (1-33 amino acids), and *At*AOC2 (1-77 amino acids) were obtained from the UniProt database. The integration of the three enzymes into the SJ05 genome, without a chloroplast localization peptide, directed them to the cytosol, resulting in strain SJ07. However, we did not detect the production of OPDA or the intermediate 13-HPOT (Fig S10). Proteomics analysis indicated that the three enzymes were successfully expressed in SJ07 (Fig S11), suggesting that one or more of the enzymes may be inactive.

Undetectable 13-HPOT in yeast expressing *At*LOX2, despite it being the primary enzyme responsible for producing the bulk of JA in *A. thaliana*[39], led us to screen for other LOXs with activity. *A. thaliana* has three other chloroplast lipoxygenases, *At*LOX3 (localization peptide: 1-52 amino acids), *At*LOX4 (localization peptide: 1-58 amino acids) and *At*LOX6 (localization peptide: 1-40 amino acids), which have been reported to convert free α-LeA into 13-HPOT[40]. We expressed the enzymes without their chloroplast localization peptides. Additionally, cytosolic *Gm*LOX1 and *Gm*LOX2 from *Glycine max* can utilize both free α-LeA and α-LeA in phospholipids for 13-HPOT production[41]. We integrated the candidate LOXs into strain SJ05 and found that *At*LOX4, *Gm*LOX1 and *Gm*LOX2 exhibited catalytic activity for de novo production of 13-HPOT from glucose (Fig 3A), whereas *At*LOX2, *At*LOX3 and *At*LOX6 did not (Fig S12). Among the active LOXs, *Gm*LOX2 expression resulted in the highest 13-HPOT production, with a titer of 5.1 mg/L (Fig 3B). Since *At*LOX4 can only use free α-LeA as a substrate, the lower production of 13-HPOT in its overexpression strain may be due to the less available α-LeA. In *A. thaliana*, Sn-1-specific phospholipase *At*DAD1 initiates JA biosynthesis by releasing α-LeA from phospholipids and plays an essential role in the regulation of JA production, as 30% of the sn-1 fatty acid is α-LeA[42, 43]. To investigate whether increasing the release of α-LeA from phospholipids could improve 13-HPOT production, we expressed *At*DAD1 without the chloroplast localization peptide. The expression of *At*DAD1 in the *At*LOX4 expressing strain (SJ14) enhanced 13-HPOT production by 34.8%, but not in the *Gm*LOX1 and *Gm*LOX2 expressing strains (Fig 3B), suggesting *At*DAD1 increased the pool of free α-LeA for utilization by *At*LOX4. Moreover, co-expression of *Gm*LOX2 and *At*LOX4 with *At*DAD1 in the SJ17 strain resulted in a further increase of 13-HPOT titer to 10.8 mg /L (Fig 3B).

After successfully producing 13-HPOT, our next goal was to produce OPDA from 13-HPOT. We introduced *At*AOS and *At*AOC2 into the genome of SJ17, resulting in strain SJ18. We found that SJ18 produced 4.9 mg/L OPDA from glucose (Fig 3C and 3D), demonstrating that *At*AOS and *At*AOC2 were actively expressed in the yeast cytosol. Although 12,13-EOT, an intermediate formed by *At*AOS, is not stable and can be spontaneously converted into by-products, such as alpha-ketol[44], we did not detect by-products in SJ18 (Fig S13), indicating that *At*AOC2 had sufficient activity to completely convert 12,13-EOT into OPDA. To determine

whether *At*AOS and *At*AOC2 were the limiting enzymes in OPDA production, we expressed them individually or in combination in SJ18. However, none of the single or combinatorial expression of *At*AOS and *At*AOC2 had a significantly positive effect on OPDA production (Fig 3D), demonstrating that *At*AOS and *At*AOC2 were not the rate-limiting steps in the OPDA synthetic pathway.

To confirm that all OPDA synthetic enzymes without chloroplast localization peptides were correctly targeted to the cytosol, we fused each enzyme with mCherry for detection, and eGFP fused with the cytosolic localized protein Pex19p was used as a positive control[45]. The green fluorescence represented the expression of eGFP, which should be distributed in the cytosol, while the red fluorescence represented the expression of mCherry. The red fluorescence of mCherry fused with *At*LOX4, *Gm*LOX2, *At*DAD1, *At*AOS or *At*AOC2 overlaid the green fluorescence (Fig 3E and Fig S14), respectively, confirming that all these enzymes were correctly targeted to the cytosol.

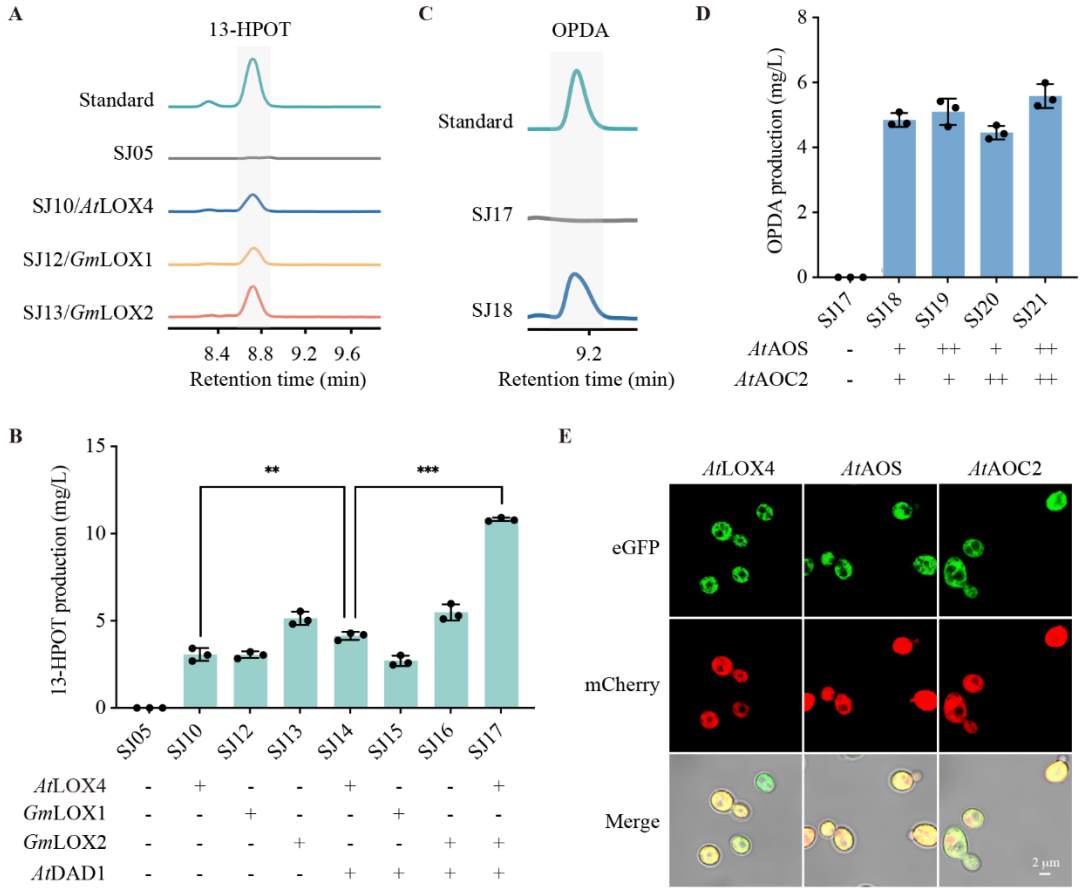

Fig 3 De novo cytosolic synthesis of OPDA in engineered yeast strains. A. 13-HPOT production in strains expressing active LOXs. B. An increase in 13-HPOT production through the introduction of phospholipase and combinatorial expression of LOXs. C. The production of OPDA from glucose. D. Bottleneck test in the OPDA synthetic pathway by individual or combinatorial expression of *At*AOS and *At*AOC2. E. Localization of OPDA biosynthetic enzymes. Statistical analysis was performed using one-tailed Student's t-test (**$p < 0.01$, ***$p < 0.001$). All data are presented as mean ± SD of biological triplicates.

De novo production of JA

We next set out to construct module III for de novo production of JA from glucose. In *Arabidopsis*, OPC-8:0 CoA Ligase 1 (OPCL1) is the only acyl-CoA synthetase (ACS) responsible for converting OPC-8:0 into OPC-8:0-CoA[46, 47]. We integrated all the required enzymes, including *At*OPR3, *At*OPCL1, *At*ACX1, *At*MFP and *At*KAT2 from *A. thaliana*, all of which included their native peroxisomal localization peptides that can be recognized by yeast[48], into the best-performing OPDA production strain SJ18. The resulting strain, SJ23, produced 9.6 mg/L JA from glucose as the sole carbon source (Fig 4A). In vitro addition of α-LeA increased JA titer to 19.0 mg/L (Fig S15). To verify that these peroxisomal enzymes were correctly distributed in the yeast peroxisome, each of them was fused to mCherry for detection, and eGFP with yeast peroxisomal localization peptide from Pex8p, a peroxisomal protein, was used as the positive control[16]. The results showed that the red dots in *At*OPR3, *At*OPCL1, *At*ACX1, *At*MFP and *At*KAT2 expressing strains overlaid the green dots (Fig 4B), revealing that all enzymes were correctly targeted into the peroxisome.

Four stereoisomers of JA are known: (−)-JA, (+)-JA, (−)-epi-JA and (+)-epi-JA[49]. In plants, the naturally produced jasmonates are (−)-JA and (+)-epi-JA. (+)-epi-JA is thermodynamically less stable and epimerizes to (−)-JA. To determine the chirality of the synthesized JA in yeast, we used semi-preparative high performance liquid chromatography (HPLC) for isolation and purification of JA (Fig S16). The chiral analysis of purified JA demonstrated that the engineered yeast strain produced all four JA stereoisomers (Fig 5C and Fig S17), indicating (+)-JA and (−)-epi-JA can also be produced by natural enzymes.

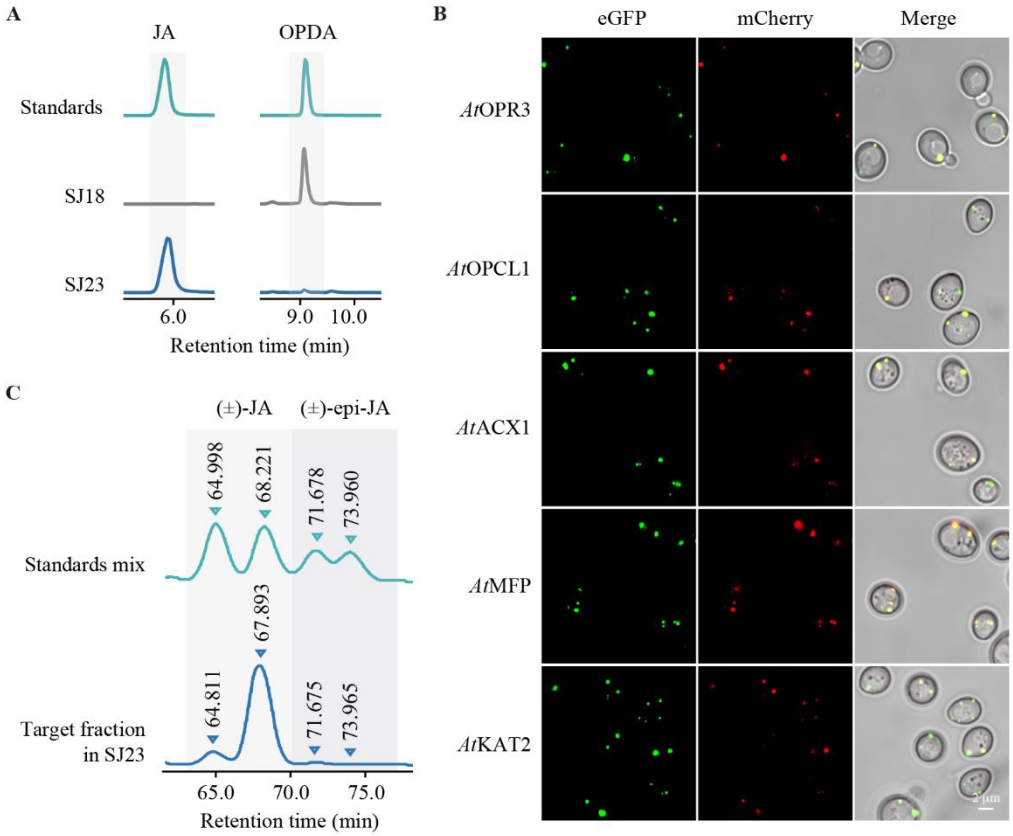

Fig 4 De novo biosynthesis of JA. A. JA production in SJ23 from glucose. B. Localization of peroxisomal enzymes. C. Chemical structures of JA produced in SJ23. All data are presented as mean ± SD of biological triplicates.

Production of JA derivatives

In plants, JA serves as an important intermediate for various modifications, forming a series of functional derivatives. Two well-known and commonly used derivatives are MeJA and JA-Ile. MeJA, a widely distributed methyl ester in the plant kingdom, is conventionally used in pre- and post-harvest fruit applications. In *A. thaliana*, MeJA is formed by the catalysis of S-adenosyl-L-methionine: jasmonic acid carboxyl methyltransferase (JMT)[50]. To produce MeJA, we integrated *At*JMT into SJ23 to construct the MeJA-producing strain SJ24. LC-MS analysis revealed that SJ24 produced 3.1 mg/L of MeJA (Fig 5A and 5B) from glucose as the sole carbon source. JA-Ile is known to be the main active JA derivative and plays an essential role in controlling vascular plant responses to herbivores[51]. JA-Ile is synthesized by the jasmonoyl-L-amino acid synthetase (JAR), which conjugates isoleucine to JA[52]. We expressed JARs from different organisms, including *A. thaliana* (*At*JAR1), *Oryza sativa* (*Os*JAR1 and *Os*JAR2), *Solanum lycopersicum* (*Sl*JAR1), *Nicotiana attenuate* (*Na*JAR4 and *Na*JAR6), in strain SJ23. All resulting strains, SJ25-SJ30, produced JA-Ile (Fig 5C), and the titers of JA-Ile from SJ26, SJ27 and SJ30 reached 7 mg/L (Fig 5D), demonstrating all selected JARs can be actively expressed in *S. cerevisiae* and that *Os*JAR1, *Os*JAR2, and *Na*JAR6 had the highest activities. The production of MeJA and JA-Ile was comparable to JA production, indicating that JA can be efficiently converted into its derivatives, and that these enzymes were not bottlenecks in the synthetic pathways.

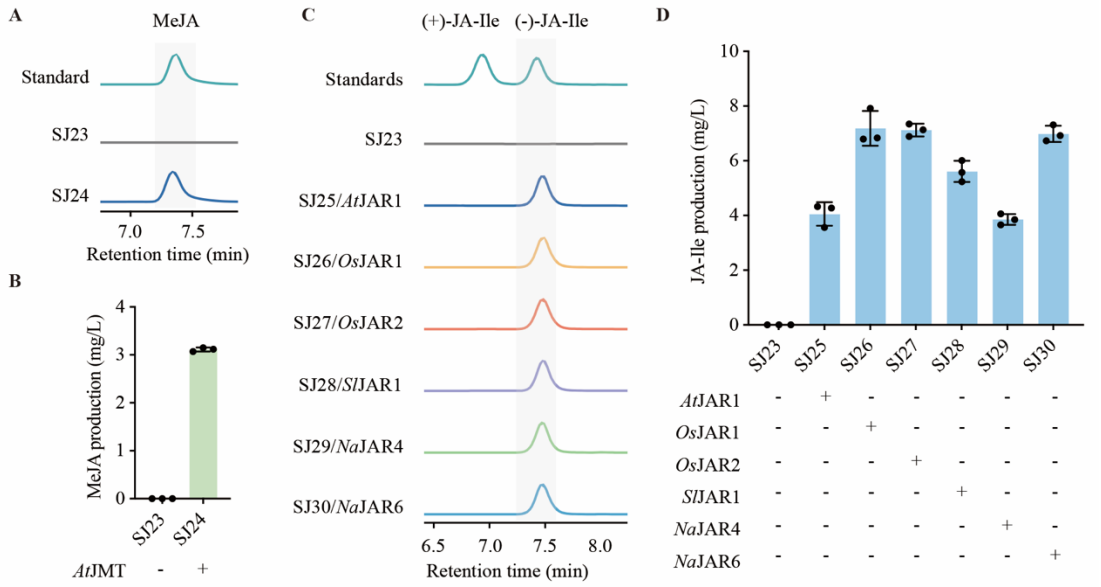

Fig 5 Biosynthesis of JA derivatives. (A) MeJA production in SJ24 from glucose. (B) The titers of MeJA produced by SJ24. (C) JA-Ile production in SJ25, SJ26, SJ27, SJ28, SJ29 and SJ30 strains from glucose. (D) The titers of JA-Ile produced by strains expressing different JAR enzymes. SJ23 was the parent strain to SJ24 and SJ25-SJ30 and was shown as the negative control. All data are presented as mean ± SD of biological triplicates.

Discussion

We have successfully engineered de novo biosynthesis of JA and its derivatives in *S. cerevisiae*, mimicking the natural process of JA production in plants. However, unlike plants,

yeast lacks chloroplasts, where α-LeA and OPDA are synthesized in plants. Therefore, we engineered the yeast ER to produce α-LeA, similar to what had been done previously, and improved its production to 50 mg/L, the highest titers produced by *S. cerevisiae* so far. We also created an OPDA synthetic pathway in the yeast cytosol, mimicking the pathway found in plant chloroplasts, thereby offering a new strategy for engineering OPDA production in other organisms.

Based on the production of precursors and jasmonates in the synthetic pathway, along with enzyme overexpression and the substrate-feeding experiments, we speculate that one of the rate-limiting steps in the JA synthetic pathway is the low production of α-LeA. In the future, attempts to increase the production of α-LeA can be made by improving the production of free fatty acids, which has been achieved through metabolic engineering strategies in *S. cerevisiae*, reaching over 30 g/L[19, 53]. In addition, the conversion of oleic acid to α-LeA occurs while these fatty acids are present as lipid-linked substrate phospholipids. Increasing the production of free oleic acid by expressing elongase *Rn*ELO2 did not lead to improvements in linoleic acid and α-LeA levels, indicating that free oleic acid production is not the limiting factor, but rather its conversion into phospholipids or insufficient activity of FAD2 and FAD3. Therefore, engineering the biosynthesis of phospholipids represents a crucial and promising approach for enhancing α-LeA production. FAD2 and FAD3 are temperature-sensitive enzymes[54], and their stability and activity may be improved by directed evolution[55, 56]. Another bottleneck is the inefficient catalytic activity of LOX. *At*LOX4 has the highest in vitro activity, while *At*LOX2, which is involved in the bulk production of JA in plants[20, 39], exhibited low activity. This may be explained by its instability in a heterologous host, as evidenced by its previous expression in insect cells to characterize its enzymatic activity[40]. Therefore, extensive screening of related native enzymes or directed evolution may be necessary to find a more preferrable LOX. Furthermore, metabolic engineering of yeast organelles has the potential to improve the production of JA and its precursors and derivatives[57]. For example, the ER could be expanded to improve enzyme activity and α-LeA production[58, 59]. In addition, peroxisome biogenesis could be stimulated[60], and peroxisomes could be engineered to increase enzyme import[61] and to enhance co-factor suppy[62].

There are four known JA stereoisomers[49], and the naturally produced JAs are (−)-JA and (+)-epi-JA, as described previously[63]. Interestingly, our engineered yeast strain produced all four JA stereoisomers (Fig 4C), demonstrating that (+)-JA and (−)-epi-JA can also be produced by natural enzymes. We suspect that the undetectable (+)-JA and (−)-epi-JA in plants may be due to their low production or the existence of enzymes that transform them into (−)-JA and (+)-epi-JA. Our yeast strain offers a clear platform for further elucidating naturally produced JA stereoisomers, which are limited by the complex background of plants.

In summary, we have successfully synthesized JA and its derivatives de novo in *S. cerevisiae* for the first time, demonstrating a significant step towards a sustainable and more efficient bioprocess than what is currently available in plants. Our engineering strategy will enable commercial-scale production of JA and its derivatives.

Materials and methods

Chemical standards and reagents

The information for all chemical standards, including CAS number and sources, was listed

in Supplementary Table S2. Kits for RNA isolation, plasmid extraction, and DNA gel purification were purchased from TIANGEN Biotech (Beijing) Co., Ltd. Phanta Max Master Mix for PCR was purchased from Vazyme Biotech (Nanjing) Co., Ltd. All-in-one First-Strand cDNA Synthesis SuperMix for RT-PCR were obtained from TransGen Biotech Co., Ltd.

DNA Cloning

The complete nucleotide sequences were obtained from the NCBI database (https://www.ncbi.nlm.nih.gov) and are listed in Supplementary Table S3. Genes from *Arabidopsis thaliana* (*At*) or *Nicotiana attenuata* (*Na*) were amplified using cDNA as the template, respectively. Those in other species such as *Kluyveromyces lactis* (*Kl*) and *Camelina sativawere* (*Cs*) were synthesized with codon optimization. DNA fragments from *S. cerevisiae* (*Sc*), including genes, promoters, terminators and flanking regions, were prepared using genomic DNA as a PCR template.

Each expression cassette for genome editing with CRISPR-Cas9 consisted of upstream homology arms (~500 nt), promoter, desired gene, terminator and downstream homology arms (~500 nt). Assembly of the pieces was achieved by fusion PCR. Specifically, primary fragments with overlapping sequences were obtained first by PCR using primers given in Supplementary Table S4. PCR products were purified and subjected to another PCR reaction without any primers to generate the full-length fusion gene. The fusion gene was then used as a template of the final PCR using primers. The resulting fusion products were then used for yeast transformation.

Guide-RNA plasmids (Supplementary Table S5) used in this study were previously constructed[16]. And plasmids for subcellular localization of target genes were designed based on the pJFE3 vector, which contains a 2μ replication origin and a *URA3* marker. Red fluorescent protein mCherry was attached to the gene of interest as an N-terminal tag. Fusion protein was then expressed under the control of *SkGAL2* promoter and *PGK* terminator. DNA fragments and linearized plasmid backbone were prepared. The construction was performed by Gibson assembly at 50°C, followed by transformation into *E. coli* DH5α. After an overnight cultivation at 37°C, the recombinant clones on LB plates with ampicillin were picked for PCR screening and verified by Sanger sequencing.

Yeast strain construction

All *S. cerevisiae* strains listed in Supplementary Table S6 were constructed using the high-efficiency LiAc/SS carrier DNA/PEG protocol. Genome editing was performed using Lab001 strain[64]. The target cassette, as repair template, together with the relevant guide-RNA plasmid were pooled for transformation. Transformants were selected on SC medium lacking the appropriate amino acid (uracil/and tryptophan). After a 3-day cultivation at 30°C, clones were randomly picked and confirmed by both diagnostic primers and sequencing. Yeasts with correct integration were cultivated in YPD medium and then plated on SC containing 5-FOA for removing guide-RNA plasmid containing *URA3* marker.

Strains used for subcellular localization determination was designed based on modified BY4742[13] that harbored an eGFP reporter with different localization peptides. Plasmids expressing the desired gene with mCherry reporter were transformed into the corresponding host. Recombinant yeasts were grown on SC medium without uracil for 3 days and then verified by colony PCR.

Yeast cultivation

Cultivation medium including nitrogen-limited minimal medium (NSD, a modified SC medium with 0.1% ammonium sulfate and 10% glucose)[24] and YPD medium (1% yeast extract, 2% peptone, 2% glucose), cultivation temperature (20/25/30°C) and incubation time (3/5/7 days) were considered in culture condition optimization for α-LeA production using strain SJ01. The best performing cultivation condition was applied to all flask fermentations for metabolite extraction. Briefly, yeast colonies were precultured in YPD medium at 30°C for 12-16 h, and then incubated into 20 mL fresh medium with an initial OD_{600} of 0.1. A volume of 3 mL filter sterilized dodecane was added for α-LeA production. In feeding experiment, different concentrations of α-LeA were added in the medium.

Yeast cells for confocal microscopy were prepared as follows. Colonies were inoculated in 2 mL SC medium containing glucose or YPD at 30°C for 24 h. Yeast cells were then pelleted by centrifugation at 4°C, washed twice with sterile water and resuspended into 10 mL fresh SC medium containing galactose or YPD to a final OD_{600} of 0.1 and cultivated for 24-36 h.

To monitor the growth of yeast strains, an overnight saturated culture was prepared and diluted into 20 mL of YPD medium with an initial OD_{600} of 0.2. Cell density was measured at various time points during a 5-day cultivation at 25°C. For temperature sensitivity tests, the saturated culture was harvested and mixed with sterile water to generate a serial dilution (1, 10^{-1}, 10^{-2}, 10^{-3}, 10^{-4}). Then, 2 μL of each dilution was spotted onto a YPD agar plate and incubated at various temperature (16°C, 25°C, 30°C, 37°C, 42°C) for 72 h. In ethanol tolerance assays, the dilutions were plated on YPD agar plates containing ethanol at various concentrations (0%, 2%, 4%, 8%, 10% and 12%) and cultivated at 25°C for 72 h.

Metabolite extraction

The intracellular fatty acid contents were determined by intracellular total fatty acid analysis[24]. To achieve the esterification of fatty acids, yeast cells were harvested from 5 mL cultures by centrifugation, washed using water, and hydrolyzed in 1 mL 10% methanolic HCl and 0.5 mL dichloromethane at 60°C for 3 h. The resulting fatty acid methyl esters were then extracted using 2 mL saturated NaCl solution and 1 mL hexane after which the upper phase was removed and evaporated until dryness. For the content determination of extracellular free fatty acid, a method was used as described previously[65]. After two-phase cultivation, the culture broth and dodecane layer were separated by centrifugation, and 200 μL dodecane was transferred and treated with 2 mL boron trifluoride-methanol solution at 60°C for 1 h to form esters derivatives. The tubes were then cooled to room temperature, and fatty acid methyl esters were extracted using 2 mL Milli-Q H_2O and 2 mL hexane. The upper organic phase was collected and evaporated, and the dried extracts were redissolved in hexane before gas chromatography-mass spectrometry (GC-MS) analysis. In addition, a protocol for membrane fatty acid analysis was developed, starting with membrane extraction[66]. Initially, cell pellets obtained from 30 mL culture were collected and washed twice with PBS buffer. Subsequently, the pellets were resuspended in 2 mL of homogenization buffer (250 mM sucrose, 1 mM EDTA and 10 mM Tris, pH to 7.2) and subjected to glass bead vertexing at 4°C. The homogenate was then centrifuged at 700 ×g for 10 min to remove cell debris, and the resulting supernatant was transferred for ultracentrifugation (100, 000 ×g, 1 h, 4°C). After centrifugation, supernatant was carefully discarded while pellet was collected and washed (100, 000 ×g, 1 h, 4°C). The extracted pellet was subjected to transesterification using 10% methanolic HCl. Transesterification of isolated lipids to fatty acid methyl esters was used for quantitation via GC-MS.

For the extraction of 13-HPOT, OPDA, JA and JA derivatives, a method established by Pan[67] was used. Briefly, 1 mL of cell cultures were collected and mixed with 500 μL of extraction solvent (2-propanol/H_2O/concentrated HCl=2:1:0.02, v/v/v). We then subjected the mixture to glass bead vortexing and ultrasonication at 4°C. Next, 1 mL of dichloromethane was added to the sample and shaken for 5 min. After centrifugation, the lower phase was collected and concentrated with nitrogen flow. The dried samples were dissolved in methanol and injected for liquid chromatography/-mass spectrometry (LC/-MS) analysis.

Chemical analysis

Quantitative analysis of fatty acid methyl esters was performed on an 8890 GC system (Agilent, US) equipped with a HP-5ms Ultra Inert column (0.25 mm*30 m, 0.25 μm, Agilent, US) and a 7000D triple quadrupole mass spectrometer (Agilent, US). The column temperature was set as follows: started at 150°C; ramped to 280°C at a rate of 20°C/min and held for 4 min. The temperature of injector and detector were both set at 280°C. Data were acquired in SIM mode, with real-time monitoring of respective molecular ions m/z 292 (α-LeA), m/z 294 (linoleic acid), m/z 296 (oleic acid), m/z 298 (stearic acid), m/z 268 (palmitoleic acid) and m/z 270 (hexadacanoic acid). DB-FFAP column (0.25 mm*30 m, 0.25 μm, Agilent, US) was used for complete separation of fatty acid methyl esters. The initial temperature was set at 60°C for 2 min, then raised to 150°C at a rate of 10°C/min and held for 10 min. The temperature was then increased to 230°C at a rate of 20°C/min and held for 5 min. The temperature of the inlet and EI source was maintained at 260°C and 280°C, respectively.

Detection of 13-HPOT, OPDA, JA and JA derivatives was carried out using a 1290 Infinity II LC system (Agilent, US) coupled with a 6470 triple quadrupole mass spectrometer (Agilent, US). Samples were eluted on a Poroshell 120 EC-C18 column (3 mm*100 mm, 2.7 μm, Agilent, US) with a flow rate of 0.2 mL/min at 30°C for 15 min. The mobile phase was composed of Milli-Q H_2O with 0.1% (v/v) formic acid (solvent A) and methanol containing 0.1% (v/v) formic acid (solvent B). The gradient profile was as follows: a linear gradient of 60 to 95% B for 5 min, held at 95% B for 3 min, returned to initial conditions of 60% B at 8.1 min and maintained for 7 min. All quantifications were performed using MRM mode. The MRM transitions for each metabolite were optimized and listed in Supplemental Table S7.

The purification of JA was performed using a Semi-Preparative HPLC platform (Agilent, US) equipped with a 1260 Infinity II system, a UV/Vis diode array detector (DAD), and a fraction collection. The column Eclipse XDB-C18 (9.4 mm*250 mm, 5 μm, Agilent, US) was used for separation under an elution rate of 3 mL/min and the gradient program was set as mentioned above. The fraction containing JA peak, which eluted between 5.95 and 6.59 min with a UV maximum of 205 nm, was automatically collected and dried under nitrogen atmosphere. The resulting residue was dissolved in hexane and subjected to normal phase chiral separation.

An Agilent 1100 series HPLC system (Agilent, US) equipped with a DAD detector was used to identify JA stereoisomers. Chiral separation was conducted on a CHIRALCEL OD-H column (4.6*250 mm, 5 μm, Daicel, Japan) at a flow rate of 0.2 mL/min at 30°C for 120 min. The mobile phase comprised 97% hexane and 3% isopropanol with 0.1% (v/v) trifluoroacetic acid. A detection wavelength of 205 nm was selected for the analysis.

Fluorescence microscopy

Yeast cells were washed with PBS buffer and were subsequently diluted to a final OD_{600}

of 5.0. Sample (10 μL) was carefully applied to an objective slide and covered with a cover slip. Fluorescence and bright field images were captured with an inverted confocal microscope A1R (Nikon, Japan) using the oil-immersed (100X) objective lens. GFP was excited by 488 nm laser line, while mCherry was by 561 nm. The NIS-Elements software was used for image capturing, analysis and processing.

Lipidomic analysis

Total lipids were extracted from yeast pellets using a methyl-tert-butyl ether (MTBE) /methanol/water solvent system[68]. Briefly, a volume of 1 mL methanol containing 80% MTBE was added to the mixture of collected cells and internal standard. After 20 min of sonication and a 30-min standing period, the sample was mixed with 200 μL Milli-Q H_2O and centrifuged at 14,000 rpm for 15 min. The upper organic phase was then transferred and dried. Lipid extracts were resuspended in 200 μL isopropanol/acetonitrile (9:1, v/v) prior to analysis by ultra high-performance liquid chromatography system UHPLC Nexera LC-30A. Both Kinetex C18 column (2.1 mm*100 mm, 2.6 μm, Phenomenex, US) and Luna NH_2 column (2.0 mm*100 mm, 3.0 μm, Phenomenex, US) were used for separation. The mobile phase system for C18 column was as follows: acetonitrile/water (90:30, v/v) containing 5 mM ammonium acetate (solvent A) and isopropanol (solvent B); 0-5.0 min 20% to 60% B; 5.0-13.0 min 60% to 100% B; 13.1-17.0 min 20% B. Separation was carried out at 45°C with a flow rate of 0.35 mL/min. While NH_2 column achieved its separation by using the following conditions: column temperature of 40°C; flow rate of 0.4 mL/min; methanol/acetonitrile (50:50, v/v) containing 2 mM ammonium acetate for solvent A; acetonitrile/water (50:50, v/v) containing 2 mM ammonium acetate for solvent B; 0-3.0 min 3% B; 3.0-13.0 min 3% to 100% B; 13.0-17.0 min 100% B; 17.1-22.0 min 3% B. The AB SCIEX Triple Quad 6500 and QTRAP mass spectrometer equipped with an electrospray ionization (ESI) source was used for the detection of lipids in both positive and negative modes. Raw MS data were processed with Sciex OS software.

Proteomic analysis

Protein extracts were prepared as previously described. In brief, the harvested cells were resuspended in 50 mM NH_4HCO_3 with 8 M urea and then mechanically broke. Protein concentration of supernatant was determined by BCA protein assay kit (Solarbio, China). 100 μg proteins were used for digestion and the resulting tryptic peptides were desalted on C18 Sep-Pak cartridges (Welch, China), and dried prior to LC-MS/MS analyses. For LC-MS/MS analysis, samples were reconstituted in an aqueous solution containing 0.1% FA. Peptide samples were subjected to an Ultimate™ 3000 RSLCnano system (Thermo Scientific, US) coupled to a Q-Exactive™ HF Orbitrap mass spectrometer (Thermo Fisher Scientific, US). Peptides were loaded onto a 3 μm*0.2 cm pre-column (P/N 164535, Thermo Scientific, US) and separated on a 2 μm*15 cm capillary column (P/N 164534, Thermo Scientific, US). The mass spectrometer was operated in data-dependent mode with a full MS scan (350–2000 m/z) at a resolution of 60,000 followed by HCD (Higher Collisional Dissociation) fragmentation at normalized collision energy of 28%. The MS2 automatic gain control (AGC) target was set to 5E4 with a maximum injection time (MIT) of 50 ms, and dynamic exclusion was set to 30 s.

Acknowledgements

This work was financially supported by National Key Research and Development Program of China (2018YFA0903200), the National Natural Science Foundation of China (32071421),

Guangdong Basic and Applied Basic Research Foundation (2021A1515010842), Shenzhen Science and Technology Program (ZDSYS20210623091810032 and RCYX20200714114736026). We thank Tao. Yu for critical discussion, and the SIAT Mass Spectrometry Infrastructure for assistance with metabolite analysis. We would like to thank CHI BIOTECH CO., LTD. for assisting in the metabolite and bioinformatics analyses.

Author contributions

J.D.K. conceived this study. H.T., X.L. S.L. and J.D. designed and performed the experiments, analyzed the data, and drafted the manuscript. J.D.K. revised the manuscript. All authors revised and approved the manuscript.

Competing interests

J.D.K. has a financial interest in Amyris, Lygos, Demetrix, Napigen, Maple Bio, Apertor Labs, Zero Acre Farms, Berkeley Yeast, and Ansa Biotechnology. X.L. has a financial interest in Demetrix. All other authors declare no competing interests.

Data availability

Source data are provided with this paper.

References

1. Wang, J., Song, L., Gong, X., Xu, J. & Li, M. Functions of jasmonic acid in plant regulation and response to abiotic stress. *Int J Mol Sci* **21**, 1446 (2020).
2. Yukimune, Y., Tabata, H., Higashi, Y. & Hara, Y. Methyl jasmonate-induced overproduction of paclitaxel and baccatin III in Taxus cell suspension cultures. *Nat. Biotechnol* **14**, 1129-1132 (1996).
3. Deepthi, S. & Satheeshkumar, K. Cell line selection combined with jasmonic acid elicitation enhance camptothecin production in cell suspension cultures of Ophiorrhiza mungos L. *Appl. Microbiol. Biotechnol.* **101**, 545-558 (2017).
4. Shen, Z. et al. High production of jasmonic acid by Lasiodiplodia iranensis using solid-state fermentation: optimization and understanding. *Biotechnol J* **17**, 2100550 (2022).
5. Scognamiglio, J., Jones, L., Letizia, C.S. & Api, A.M. Fragrance material review on methyl jasmonate. *Food Chem. Toxicol.* **50 Suppl 3**, S572-576 (2012).
6. Sá-Nakanishi, A.B. et al. Anti-inflammatory and antioxidant actions of methyl jasmonate are associated with metabolic modifications in the liver of arthritic rats. *Oxid. Med. Cell. Longev* **2018**, 2056250 (2018).
7. Fingrut, O. & Flescher, E. Plant stress hormones suppress the proliferation and induce apoptosis in human cancer cells. *Leukemia* **16**, 608-616 (2002).
8. Bömer, M. et al. Jasmonates induce Arabidopsis bioactivities selectively inhibiting the growth of breast cancer cells through CDC6 and mTOR. *New Phytol.* **229**, 2120-2134 (2021).
9. Creelman, R.A. & Mullet, J.E. Jasmonic acid distribution and action in plants: regulation during development and response to biotic and abiotic stress. *Proc. Natl. Acad. Sci. U. S. A.* **92**, 4114-4119 (1995).
10. Ghasemi Pirbalouti, A., Sajjadi, S.E. & Parang, K. A review (research and patents) on

jasmonic acid and its derivatives. *Arch. Pharm. (Weinheim)* **347**, 229-239 (2014).
11. Chapuis, C. The jubilee of methyl jasmonate and hedione®. *Helv. Chim. Acta* **95**, 1479-1511 (2012).
12. Carroll, A.L., Desai, S.H. & Atsumi, S. Microbial production of scent and flavor compounds. *Curr. Opin. Biotechnol.* **37**, 8-15 (2016).
13. Eng, F. et al. Jasmonic acid biosynthesis by fungi: derivatives, first evidence on biochemical pathways and culture conditions for production. *PeerJ* **9**, e10873 (2021).
14. Borodina, I. & Nielsen, J. Advances in metabolic engineering of yeast Saccharomyces cerevisiae for production of chemicals. *Biotechnol J* **9**, 609-620 (2014).
15. Sheng, J. & Feng, X. Metabolic engineering of yeast to produce fatty acid-derived biofuels: bottlenecks and solutions. *Front. Microbiol.* **6**, 554 (2015).
16. Reider Apel, A. et al. A Cas9-based toolkit to program gene expression in Saccharomyces cerevisiae. *Nucleic Acids Res.* **45**, 496-508 (2017).
17. Mans, R. et al. CRISPR/Cas9: a molecular Swiss army knife for simultaneous introduction of multiple genetic modifications in Saccharomyces cerevisiae. *FEMS Yeast Res.* **15** (2015).
18. Jakočiūnas, T. et al. Multiplex metabolic pathway engineering using CRISPR/Cas9 in Saccharomyces cerevisiae. *Metab. Eng.* **28**, 213-222 (2015).
19. Yu, T. et al. Reprogramming yeast metabolism from alcoholic fermentation to lipogenesis. *Cell* **174**, 1549-1558.e1514 (2018).
20. Pollmann, S. et al. Substrate channeling in oxylipin biosynthesis through a protein complex in the plastid envelope of Arabidopsis thaliana. *J. Exp. Bot.* **70**, 1483-1495 (2019).
21. Wasternack, C. & Hause, B. The missing link in jasmonic acid biosynthesis. *Nat. Plants* **5**, 776-777 (2019).
22. Theodoulou, F.L. et al. Jasmonic acid levels are reduced in COMATOSE ATP-binding cassette transporter mutants. Implications for transport of jasmonate precursors into peroxisomes. *Plant Physiol.* **137**, 835-840 (2005).
23. Li, C. et al. Role of beta-oxidation in jasmonate biosynthesis and systemic wound signaling in tomato. *Plant Cell* **17**, 971-986 (2005).
24. Kainou, K., Kamisaka, Y., Kimura, K. & Uemura, H. Isolation of Δ12 and ω3-fatty acid desaturase genes from the yeast Kluyveromyces lactis and their heterologous expression to produce linoleic and α-linolenic acids in Saccharomyces cerevisiae. *Yeast* **23**, 605-612 (2006).
25. Zhang, H.T., Yang, J.S., Shan, L. & Bi, Y.P. Functional expression of a ω-3 fatty acid desaturase gene from Glycine max in Saccharomyces cerevisiae. *Chinese J. Biotechnol.* **22**, 33-38 (2006).
26. Xue, Y. et al. Omega-3 fatty acid desaturase gene family from two ω-3 sources, Salvia hispanica and Perilla frutescens: cloning, characterization and expression. *PLoS One* **13**, e0191432 (2018).
27. Rodríguez-Rodríguez, M.F., Salas, J.J., Venegas-Calerón, M., Garcés, R. & Martínez-Force, E. Molecular cloning and characterization of the genes encoding a microsomal oleate Δ12 desaturase (CsFAD2) and linoleate Δ15 desaturase (CsFAD3) from Camelina sativa. *Ind Crops Prod* **89**, 405-415 (2016).

28. Oura, T. & Kajiwara, S. Saccharomyces kluyveri FAD3 encodes an omega3 fatty acid desaturase. *Microbiology (Reading, Engl)* **150**, 1983-1990 (2004).
29. Sibirny, A.A. Yeast peroxisomes: structure, functions and biotechnological opportunities. *FEMS Yeast Res.* **16**, fow038 (2016).
30. Yazawa, H., Iwahashi, H., Kamisaka, Y., Kimura, K. & Uemura, H. Production of polyunsaturated fatty acids in yeast Saccharomyces cerevisiae and its relation to alkaline pH tolerance. *Yeast* **26**, 167-184 (2009).
31. Yazawa, H., Iwahashi, H., Kamisaka, Y., Kimura, K. & Uemura, H. Improvement of polyunsaturated fatty acids synthesis by the coexpression of CYB5 with desaturase genes in Saccharomyces cerevisiae. *Appl. Microbiol. Biotechnol.* **87**, 2185-2193 (2010).
32. Yazawa, H. et al. Heterologous production of dihomo-gamma-linolenic acid in Saccharomyces cerevisiae. *Appl. Environ. Microbiol.* **73**, 6965-6971 (2007).
33. Oura, T. & Kajiwara, S. Substrate specificity and regioselectivity of delta12 and omega3 fatty acid desaturases from Saccharomyces kluyveri. *Biosci. Biotechnol. Biochem.* **72**, 3174-3179 (2008).
34. Ferreira, R., Teixeira, P.G., Siewers, V. & Nielsen, J. Redirection of lipid flux toward phospholipids in yeast increases fatty acid turnover and secretion. *Proc. Natl. Acad. Sci. U. S. A.* **115**, 1262-1267 (2018).
35. Bonner, W.M. & Bloch, K. Purification and properties of fatty acyl thioesterase I from Escherichia coli. *J. Biol. Chem.* **247**, 3123-3133 (1972).
36. Paton, C.M. & Ntambi, J.M. Biochemical and physiological function of stearoyl-CoA desaturase. *Am. J. Physiol. Endocrinol. Metab.* **297**, E28-37 (2009).
37. Yazawa, H., Kamisaka, Y., Kimura, K., Yamaoka, M. & Uemura, H. Efficient accumulation of oleic acid in Saccharomyces cerevisiae caused by expression of rat elongase 2 gene (rELO2) and its contribution to tolerance to alcohols. *Appl. Microbiol. Biotechnol.* **91**, 1593-1600 (2011).
38. Zhai, Q., Yan, C., Li, L., Xie, D. & Li, C. Hormone metabolism and signaling in plants. (eds. J. Li, C. Li & S.M. Smith) 243-272 (Academic Press, 2017).
39. Chauvin, A., Caldelari, D., Wolfender, J.L. & Farmer, E.E. Four 13-lipoxygenases contribute to rapid jasmonate synthesis in wounded Arabidopsis thaliana leaves: a role for lipoxygenase 6 in responses to long-distance wound signals. *New Phytol.* **197**, 566-575 (2013).
40. Bannenberg, G., Martínez, M., Hamberg, M. & Castresana, C. Diversity of the enzymatic activity in the lipoxygenase gene family of Arabidopsis thaliana. *Lipids* **44**, 85-95 (2009).
41. Mandal, S., Dahuja, A. & Santha, I.M. Lipoxygenase activity in soybean is modulated by enzyme-substrate ratio. *J. Plant Biochem. Biotechnol.* **23**, 217-220 (2014).
42. Browse, J., Warwick, N., Somerville, C.R. & Slack, C.R. Fluxes through the prokaryotic and eukaryotic pathways of lipid synthesis in the '16:3' plant Arabidopsis thaliana. *Biochem. J* **235**, 25-31 (1986).
43. Ishiguro, S., Kawai-Oda, A., Ueda, J., Nishida, I. & Okada, K. The DEFECTIVE IN ANTHER DEHISCIENCE gene encodes a novel phospholipase A1 catalyzing the initial step of jasmonic acid biosynthesis, which synchronizes pollen maturation, anther dehiscence, and flower opening in Arabidopsis. *Plant Cell* **13**, 2191-2209 (2001).

44. Löwe, J., Dietz, K.J. & Gröger, H. From a biosynthetic pathway toward a biocatalytic process and chemocatalytic modifications: three-step enzymatic cascade to the plant metabolite cis-(+)-12-OPDA and metathesis-derived products. *Adv. Sci.* **7**, 1902973 (2020).
45. Huh, W.K. et al. Global analysis of protein localization in budding yeast. *Nature* **425**, 686-691 (2003).
46. Koo, A.J.K., Chung, H.S., Kobayashi, Y. & Howe, G.A. Identification of a peroxisomal Acyl-activating enzyme involved in the biosynthesis of jasmonic acid in Arabidopsis. *J. Biol. Chem.* **281**, 33511-33520 (2006).
47. Wasternack, C. & Kombrink, E. Jasmonates: structural requirements for lipid-derived signals active in plant stress responses and development. *ACS Chem. Biol.* **5**, 63-77 (2010).
48. Kragler, F., Lametschwandtner, G., Christmann, J., Hartig, A. & Harada, J.J. Identification and analysis of the plant peroxisomal targeting signal 1 receptor NtPEX5. *Proc. Natl. Acad. Sci. U. S. A.* **95**, 13336-13341 (1998).
49. Koch, T., Bandemer, K. & Boland, W. Biosynthesis of cis-jasmone: a pathway for the inactivation and the disposal of the plant stress hormone jasmonic acid to the gas phase? *Helv. Chim. Acta* **80**, 838-850 (1997).
50. Seo, H.S. et al. Jasmonic acid carboxyl methyltransferase: a key enzyme for jasmonate-regulated plant responses. *Proc. Natl. Acad. Sci. U. S. A.* **98**, 4788-4793 (2001).
51. Fu, W. et al. The jasmonic acid-amino acid conjugates JA-Val and JA-Leu are involved in rice resistance to herbivores. *Plant Cell Environ.* **45**, 262-272 (2022).
52. Suza, W.P. & Staswick, P.E. The role of JAR1 in Jasmonoyl-L-isoleucine production during Arabidopsis wound response. *Planta* **227**, 1221-1232 (2008).
53. Yu, T. et al. Metabolic reconfiguration enables synthetic reductive metabolism in yeast. *Nat. Metab.* **4**, 1551-1559 (2022).
54. Dar, A.A., Choudhury, A.R., Kancharla, P.K. & Arumugam, N. The FAD2 gene in plants: occurrence, regulation and role. *Front. Plant Sci.* **8**, 1789 (2017).
55. Wang, Y. et al. Directed evolution: methodologies and applications. *Chem. Rev.* **121**, 12384-12444 (2021).
56. Romero, P.A. & Arnold, F.H. Exploring protein fitness landscapes by directed evolution. *Nat. Rev. Mol. Cell Bio.* **10**, 866-876 (2009).
57. Hammer, S.K. & Avalos, J.L. Harnessing yeast organelles for metabolic engineering. *Nat. Chem. Biol.* **13**, 823-832 (2017).
58. Kim, J.E. et al. Tailoring the Saccharomyces cerevisiae endoplasmic reticulum for functional assembly of terpene synthesis pathway. *Metab. Eng.* **56**, 50-59 (2019).
59. Arendt, P. et al. An endoplasmic reticulum-engineered yeast platform for overproduction of triterpenoids. *Metab. Eng.* **40**, 165-175 (2017).
60. Zhou, Y.J. et al. Harnessing yeast peroxisomes for biosynthesis of fatty-acid-derived biofuels and chemicals with relieved side-pathway competition. *J. Am. Chem. Soc.* **138**, 15368-15377 (2016).
61. DeLoache, W.C., Russ, Z.N. & Dueber, J.E. Towards repurposing the yeast peroxisome for compartmentalizing heterologous metabolic pathways. *Nat. Commun.* **7**, 11152 (2016).

62. Liu, G.S. et al. The yeast peroxisome: a dynamic storage depot and subcellular factory for squalene overproduction. *Metab. Eng.* **57**, 151-161 (2020).
63. Jarocka-Karpowicz, I. & Markowska, A. Therapeutic potential of jasmonic acid and its derivatives. *Int. J. Mol. Sci.* **22**, 8437 (2021).
64. Zheng, T. et al. Upcycling CO2 into energy-rich long-chain compounds via electrochemical and metabolic engineering. *Nat. Catal.* **5**, 388-396 (2022).
65. Kim, S. & Gonzalez, R. Selective production of decanoic acid from iterative reversal of β-oxidation pathway. *Biotechnol. Bioeng.* **115**, 1311-1320 (2018).
66. Smith, S.M. Strategies for the purification of membrane proteins. *Methods Mol. Biol.* **1485**, 389-400 (2017).
67. Pan, X., Welti, R. & Wang, X. Quantitative analysis of major plant hormones in crude plant extracts by high-performance liquid chromatography-mass spectrometry. *Nat. Protoc.* **5**, 986-992 (2010).
68. Luzarowski, M. et al. Global mapping of protein–metabolite interactions in Saccharomyces cerevisiae reveals that Ser-Leu dipeptide regulates phosphoglycerate kinase activity. *Commun. Biol.* **4**, 181 (2021).